Influence of Counter-Ions on the Crystal Structures of DNA Decamers: Binding of $[Co(NH_3)_6]^{3+}$ and Ba^{2+} to A-DNA

Yi-Gui Gao,* Howard Robinson,* Jacques H. van Boom,‡ and Andrew H.-J. Wang*
*Division of Biophysics and Department of Cell and Structural Biology, University of Illinois at Urbana-Champaign, Urbana, Illinois 61801 USA, and ‡Leiden Institute of Chemistry, Gorlaeus Laboratory, 2300 RA Leiden, The Netherlands

ABSTRACT A-DNA is a stable alternative right-handed double helix that is favored by certain sequences (e.g., $(dG)_n \cdot (dC)_n$) or under low humidity conditions. Earlier A-DNA structures of several DNA oligonucleotides and RNA·DNA chimeras have revealed some conformational variation that may be the result of sequence-dependent effects or crystal packing forces. In this study, four crystal structures of three decamer oligonucleotides, d(ACCGGCCGGT), d(ACCCGCGGGT), and r(GC)d(GTATACGC) in two crystal forms (either the $P6_122$ or the $P2_12_12_1$ space group) have been analyzed at high resolution to provide the molecular basis of the structural difference in an experimentally consistent manner. The study reveals that molecules crystallized in the same space group have a more similar A-DNA conformation, whereas the same molecule crystallized in different space groups has different (local) conformations. This suggests that even though the local structure is influenced by the crystal packing environments, the DNA molecule adjusts to adopt an overall conformation close to canonical A-DNA. For example, the six independent CpG steps in these four structures have different base-base stacking patterns, with their helical twist angles (Ω) ranging from 28° to 37°. Our study further reveals the structural impact of different counter-ions on the A-DNA conformers. $[Co(NH_3)_6]^{3+}$ has three unique A-DNA binding modes. One binds at the major groove side of a GpG step at the O6/N7 sites of guanine bases via hydrogen bonds. The other two modes involve the binding of ions to phosphates, either bridging across the narrow major groove or binding between two intra-strand adjacent phosphates. Those interactions may explain the recent spectroscopic and NMR observations that $[Co(NH_3)_6]^{3+}$ is effective in inducing the B- to A-DNA transition for DNA with $(G)_n$ sequence. Interestingly, Ba^{2+} binds to the same O6/N7 sites on guanine by direct coordinations.

INTRODUCTION

The polymorphic nature of DNA conformations is now well established and plays important roles in the functions of DNA (Sinden, 1994). The equilibrium among various conformations is dependent on a number of factors, including sequence, chemical structure (e.g., ribose versus deoxyribose), humidity, and counter-ions. Although the right-handed B-DNA double helix is considered to be the most relevant conformation in vivo, other conformations may play important biological roles. For example, the recent crystal structures of the TATA-box binding protein (TBP) complexed to the TATA-containing sequence revealed that, in the complex, the DNA adopts a highly distorted A-form conformation (Kim et al., 1993a,b). TBP is bound in the wide and shallow minor groove of the A-DNA. This is in contrast to many other protein-DNA complexes in which the proteins are found in the deep major groove of B-DNA (Steitz, 1990), although a number of proteins have recently been shown to bind in the minor groove of B-DNA (Sauer, 1995).

Considerable information has been accumulated regarding the detailed molecular structure of A-DNA through crystallographic studies of several oligonucleotides. Earlier studies on a number of DNA octamers, including d(GGCCGGCC) (Wang et al., 1982), d(GGTATACC) (Shakked et al., 1983), and d(CCCCGGGG) (Haran et al., 1987), revealed that they adopted a slightly modified A-DNA conformation in which the average base pair inclination angle (~8–10°) is significantly less than that of canonical A-DNA (~19°). Subsequent work on longer G-rich DNA decamers, including d(ACCGGCCGGT) (Frederick et al., 1989), d(GCGGGCCCGC), and d(CCCGGCCGGG) (Ramakrishnan and Sundaralingam, 1993a,b), and the dodecamers d(CCCCCGCGGGGG) (Verdaguer et al., 1991) and d(CCGTACGTACGG) (Bingman et al., 1992) showed that those duplexes resemble more closely the canonical A-DNA.

It is useful to point out that the A-DNA conformation is very similar to that of the RNA duplex, except for the additional 2′-hydroxyl groups bordering the two edges of the wide minor groove in RNA (Baeyens et al., 1995; Dock-Bergeon et al., 1989). The similarity between A-DNA and RNA was first gleaned from the three-dimensional structure of an RNA·DNA chimera r(GCG)d(TATACGC) (Wang et al., 1982) whose global conformation is essentially the same as the pure A-DNA structures mentioned above or the pure RNA duplex (Dock-Bergeon et al., 1989). The crystal structures of several additional RNA·DNA chimeras, including d(GGGTATACGC)·r(GCG)d(TATACCC), r(G)d(CGTATAGCG), d(GCGT)r(A)d(TACGC) (Egli et al., 1993), d(CCGGC)r(G)d(CCGG) (Ban et al., 1994a), and

Received for publication 6 April 1995 and in final form 23 May 1995.

Address reprint requests to Dr. Andrew Wang, Department of Cell and Structural Biology, University of Illinois, 506 Morrill Hall, 505 S. Goodwin Ave. Urbana, IL 61801. Tel.: 217-244-6637; Fax:217-244-3181; E-mail: ahjwang@uiuc.edu.

0006-3495/95/08/559/10 $2.00

r(C)d(CGGCGCCG)r(G) (Ban et al., 1994b), reaffirm this view.

It is interesting to note that most of these decamers crystallize in two space groups, the hexagonal $P6_122$ ($a = b \approx 39$ Å, $c \approx 78$ Å) and the orthorhombic $P2_12_12_1$ ($a \approx 25$ Å, $b \approx 45$ Å, $c \approx 45$–47 Å). In some cases, the same sequence crystallized in both space groups, whereas in other cases different sequences crystallized in the same space group. From this wealth of A-DNA structures, one can begin to understand the sequence-dependent conformation of A-DNA and the possible influence of lattice forces on A-DNA structure. However, many questions remain unanswered. For example, although DNA with the GpG sequence appears to have the propensity to form A-DNA, it is not strictly required. In fact, d(CCGGCGCCGG) crystallized unexpectedly in the B-DNA conformation (Heineman et al., 1992). How do different counter-ions influence the polymorphic crystal forms of a particular DNA sequence? In this paper we address these issues by solving the crystal structures of three different decamer oligonucleotides in two crystal forms (either the $P6_122$ or the $P2_12_12_1$ space group) and compare their conformations. In addition, we studied the structural impact of different counter-ions on A-DNA.

MATERIALS AND METHODS

The DNA d(ACCGGCCGGT), d(ACCCGCGGGT) and the RNA·DNA chimera r(GC)d(GTATACGC) were synthesized by using automated DNA synthesizers and purified by Sepharose S100 gel filtration column chromatography. Preparations of the various crystal forms of A-DNA listed in Table 1 follow the procedures described previously (Wang and Gao, 1990). Typically, the crystallization solution contained 4 mM DNA duplex (2.5 μl), 50 mM sodium cacodylate buffer (pH 6.5; 10 μl), 20% 2-methyl-2,4-pentanediol (2.5 μl), plus varying amounts of the counter-ions (2.5 μl). For the $[Co(NH_3)_6]^{3+}$ crystal forms of d(ACCGGCCGGT) and r(GC)d(GTATACGC), $[Co(NH_3)_6]^{3+}$ solutions (10 mM; 2.5 μl) were added to each crystallization dip and allowed to equilibrate with the reservoir. Additional amounts of the $[Co(NH_3)_6]^{3+}$ were added to each crystallization dip after the crystals had appeared and stopped growing. The crystals were allowed to soak in the solution for several more days depending upon crystal stability and color change. This process ensured that the binding of metal ions had reached maximal occupancy. The $[Co(NH_3)_6]^{3+}$-containing crystals have light to medium yellow color. For the Ba^{2+} crystal form of d(ACCCGCGGGT), Ba^{2+} solutions (25 mM; 2.5 μl) were added to each crystallization dip. For the spermine crystal form of d(ACCGGCCGGT), spermine^{4+} solutions (10 mM) (2.5 μl) were added to each crystallization dip.

Suitable crystals were chosen and mounted individually in a thin-walled glass capillary and sealed with a droplet of the crystallization mother liquor for data collection. The diffraction data sets were collected at ambient room temperature (~25°C) to a resolution of 1.9 Å as indicated in Table 1. We used a Rigaku R-AXIS IIc image plate system mounted on an RU-200 rotating-anode x-ray generator at a power of 50 kV and 80 mA for data collection. The fine-focused x-ray beam (0.3 mm) was collimated with a graphite monochromator to produce the CuK_O radiation (1.5418 Å). The image plate to crystal distance was 90 mm. Forty-five and sixty frames of oscillation data (2°/10 min) were collected to cover a range of 90° and 120° of the ϕ angle for the $P2_12_12_1$ form and the $P6_122$ form, respectively. After data processing with the Molecular Structure Corporation (Woodlands, TX) software package, each data set produced a two- to fourfold redundancy in the observed reflections for both crystal forms. The R_{merge} (for all $F_o > 1.0\ \sigma F_o$ reflections) values of the data sets range from 5.3 to 6.6% (Table 1). Care was taken to account for intensity saturation on the image plate for strong reflections. Some frames were recollected with a faster oscillation speed (2°/2 min) to recover those strong (saturated) reflections. For structural refinement, only reflections with $F_o > 4.0\ \sigma F_o$ were used. Our experience with the data from the R-AXIS II image plate system showed that they tend to underestimate the background, resulting in a greater number of weak reflections. Nevertheless, even with this cutoff level, the number of reflections obtained from our area detector is still far greater than that obtained from the Rigaku AFC-5R diffractometer (for reflections with $F_o > 2.0\ \sigma F_o$) in our laboratory.

The atomic coordinates from the canonical crystal structures were used as the starting models for the refinement using the Konnert-Hendrickson constrained refinement procedure (Hendrickson and Konnert, 1979; Westhof et al., 1985). For the $P6_122$ and the $P2_12_12_1$ crystals, the coordinates from the Mg^{2+} form of d(ACCGGCCGGT) (Frederick et al., 1989) and the Mg^{2+} form of r(GCG)d(TATACGC) (Wang et al., 1982), respectively, were used with the sequence of the molecule suitably changed. To minimize the bias due to the starting model, we always started the refinement by using only the low resolution data (5 Å) with tight geometric constraints. This allowed the molecule to adjust its global conformation more correctly. The resolution was gradually increased to include more

TABLE 1 Crystal data and refinement data of three A-DNA decamers with various counter-ions

DNA	d(ACCCGCGGGT)	d(ACCGGCCGGT)	d(ACCGGCCGGT)	r(GC)d(GTATACGC)
Unit cell dimensions (Å)	$a = 40.12$	$a = 39.06$	$a = 24.73$	$a = 25.24$
	$b = 40.12$	$b = 39.06$	$b = 45.13$	$b = 44.56$
	$c = 78.22$	$c = 77.55$	$c = 47.52$	$c = 45.30$
	$\gamma = 120°$	$\gamma = 120°$		
Counter-ion	Ba^{2+}	$Co(NH_3)_6^{3+}$	Spermine^{4+}	$Co(NH_3)_6^{3+}$
Space group	$P6_122$	$P6_122$	$P2_12_12_1$	$P2_12_12_1$
V_{asym} (Å^3)	9,086	8,539	13,259	12,737
V/bp (Å^3)	1,817	1,708	1,326	1,274
Asymmetric unit	1 strand	1 strand	1 duplex	1 duplex
Unique data*	1,811	2,163	3,156	3,720
Resolution (Å)	2.00	1.90	1.90	1.90
R_{merge} (%)‡	6.5	6.6	5.3	6.4
rmsd (Å)§	0.025	0.021	0.017	0.016
Final R-values	0.206	0.194	0.200	0.182
No. of solvent	48	65	85	72

* Data ($>4\ \sigma\ F_o$) collected on R-AXIS IIc image plate area detector system at 25°C.

‡ $R_{merge} = \Sigma\,|\,I - \langle I\rangle\,|\,/\Sigma\langle I\rangle$.

§ The rmsd from ideal bond length, resulting from the restrained refinement.

data. After many cycles of refinement with all available data, the R-factor in general reached ~30% at 1.9 Å resolution. If the metal ion in the crystal lattice had a reasonable occupancy, it could be easily located from the Fourier ($2F_o - F_c$) maps. Inclusion of the metal ion(s) normally reduced the R-factor by approximately 5 to 8%, depending on the number of metal ion sites and how well ordered they were. Water molecules were then located from subsequent Fourier ($2F_o - F_c$) maps and added to the refinement. The final crystallographic R-factor was near 20%.

We have found that the occupancies of metal ions are not 100%. If the metal ions were assigned with a full occupancy, their temperature factor became very high. We therefore assigned a 50% occupancy for the metal ions so that their B-factors are comparable with the first shell water molecules (~35–50 Å^2). The crystallographic data along with the refinement results are summarized in Table 1. A total of four new structures have been analyzed. A sample electron density map of the C4 residue of the d(ACCCGCGGGT) (Ba^{2+} form) structure is shown in Fig. 1, which illustrates the correctness of the sequence. The final atomic coordinates of the structure have been deposited at the Brookhaven Protein Data Bank.

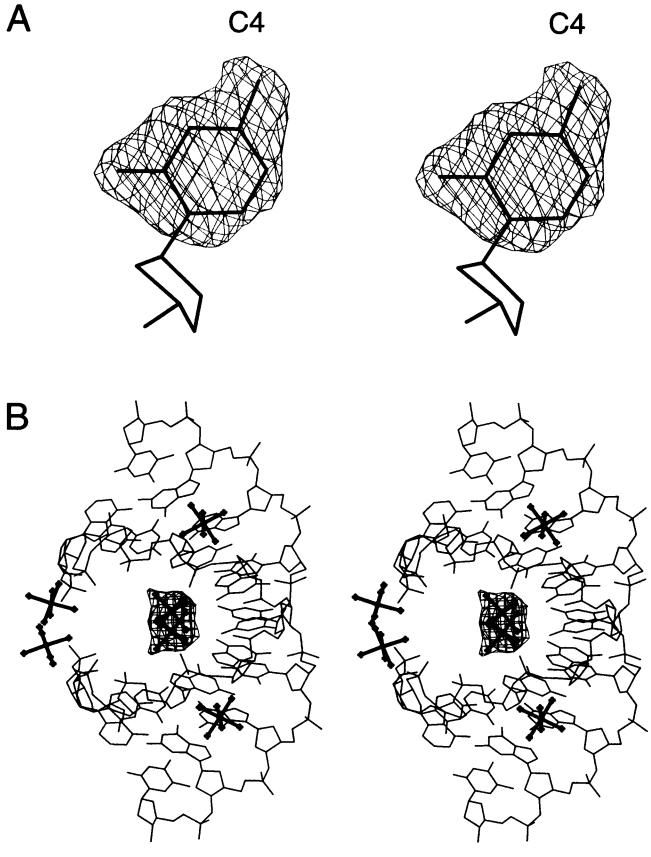

FIGURE 1 A portion of the difference ($F_o - F_c$) Fourier maps of the $P6_122$ crystals. (*A*) The C4 cytosine base from the Ba^{2+} form of the d(ACCCGCGGGT) A-DNA crystal structure. (*B*) One of the $[Co(NH_3)_6]^{3+}$ binding sites near the center of the d(ACCGGCCGGT) duplex. The electron density map suggests that two partially occupied $[Co(NH_3)_6]^{3+}$ ions are located at the edges of the G4-G5 and the symmetry-related G4*-G5* bases. Throughout the paper the DNA oligonucleotides are denoted with their base sequences numbered from 1 to 10 going from the 5′ to 3′ direction in one strand and 11 to 20 in the other strand for the $P2_12_12_1$ form. In the $P6_122$ from, the two strands are equivalent and the second strand is numbered with *.

RESULTS

Conformations of A-DNA decamers

In this study, we analyzed four different crystal structures of three independent DNA decamer molecules that were crystallized with three types of counter-ions. Our results offer an excellent opportunity to examine in a consistent manner the outstanding issues mentioned in the Introduction. Specifically, we have two different DNA molecules crystallized in the same space group, i.e., d(ACCGGCCGGT) and d(ACCCGCGGGT) are in the $P6_122$ space group, whereas d(ACCGGCCGGT) and r(GC)d(TATACGC) are in the $P2_12_12_1$ space group. Conversely, we have the same d(ACCGGCCGGT) molecule crystallized in two different space groups ($P6_122$ and $P2_12_12_1$). As the experiments have been carried out under the same conditions (crystallization, data collection, refinement, etc), the comparison among different structures should have a high internal consistency. For duplexes in the $P6_122$ form, the two strands are equivalent because the molecular twofold axis coincides with the crystallographic twofold axis. In contrast, the entire duplex is in the asymmetric unit of the $P2_12_12_1$ crystal form.

Table 2 summarizes the helix parameters of the three decamers in two crystal forms along with those from earlier work. When we examine their global conformations, it is evident that they all adopt a conformation very close to the canonical A-DNA. The duplexes have the characteristic wide and shallow minor groove and the deep and narrow major groove. The averaged base pair inclination angle is in the range of 16°-19° and the averaged x-displacement of the base pairs is approximately −4.0 Å. All sugars have the N-type pucker (C3′-endo). Nevertheless, some small variations exist between the two crystal forms. The average rise per residue values in the $P6_122$ and $P2_12_12_1$ forms are 2.66 Å and 2.49 Å, respectively, whereas the x-displacements for the two respective crystal forms are −4.00 Å and −4.90 Å (Table 2).

However, despite the similar global conformations, the molecules show significant variations in their local structures. When we compare the root mean squares deviation (rmsd) among the four different structures, a clear pattern emerges. Molecules crystallized in the same space group have a more similar conformation, whereas the same molecule crystallized in different space groups has different (local) conformations. This is illustrated in Fig. 2.

Fig. 2 *A* compares the structures of d(ACCGGCCGGT) and d(ACCCGCGGGT) in the $P6_122$ form (rmsd = 0.75 Å using common atoms) and Fig. 2 *C* compares the structures of d(ACCGGCCGGT) and r(GC)d(GTATACGC) in the $P2_12_12_1$ form (rmsd = 1.00 Å using common atoms). These results clearly show that different molecules adopt the same global conformation in a particular crystal lattice, regardless of the space group. A different picture emerges when the structures of d(ACCGGCCGGT) that has been crystallized in two different space groups are compared (Fig. 2 *B*). The significant departure of the two structures is reflected in

TABLE 2 Average helical parameters of A-DNA decamers and dodecamers

	Helical twist (deg)	Base inclination (deg)	Propeller twist (deg)	Buckle (deg)	Rise/ residue (Å)	Slide (Å)	X-disp (Å)	Reference
$P6_122$ form								
d(ACCGGCCGGT) + CoHex	33.39	17.70	−15.82	0.00	2.63	−1.24	−3.89	This work
d(ACCCGCGGGT) + Ba^{2+}	32.85	16.75	−13.63	0.00	2.63	−1.42	−4.28	This work
d(ACCGGCCGGT) + Mg^{2+}	33.06	17.32	−14.49	−0.01	2.65	−1.28	−3.84	Frederick et al., 1989
d(GCGGGCCCGC)	33.40	17.30			2.72	−1.20		Ramakrishnan et al., 1993a
$P2_12_12_1$ form								
d(ACCGGCCGGT) + spermine	31.36	16.14	−7.74	2.67	2.39	−1.86	−5.47	This work
r(GC)d(GTATACGC) + CoHex	31.70	17.49	−11.21	−0.93	2.52	−1.52	−4.63	This work
r(GCG)d(TATACGC)	32.29	19.32	−11.21	−2.33	2.52	−1.38	−4.60	Wang et al., 1982
r(G)d(CGTATACGC)	33.10				2.48			Egli et al., 1993
d(GCGGGCCCGC)	32.30	16.30			2.53	−1.73		Ramakrishnan et al., 1993a
r(C)d(CGGCGCCG)r(G)	32.40	18.70	−7.60	−1.30	2.40	−1.60	−4.70	Ban et al., 1994b
Dodecamer								
d(CCCCCGCGGGGG)	32.60		−14.6		2.39	−1.75		Verdaguer et al., 1991
d(CCGTACGTACGG)	32.41	17.65	−8.82	0.00	2.55	−1.42	−4.57	Bingman et al., 1992

Nomenclature of the helical parameters follows that of EMBO Workshop (1989).

their large rmsd (1.61 Å). The main difference appears to be localized near the 5′-end (A1 to G5 and A11 to G15) in both strands, although strand 1 seems to have a larger deviation. If we used only the last five nucleotides of both strands (C6 to T10 plus C16 to T20) in the duplex for the least-squares fitting, the rmsd was reduced to 0.90 Å. This observation suggests that the reason for the conformational difference is related to the lattice interactions between DNA molecules, which are described below.

Duplex-duplex interactions in crystals

To visualize the interactions in more detail, we show expanded views in Fig. 3, *A* and *B*, which displays the packing interactions of the A-DNA duplexes of d(ACCGGCCGGT) ($P6_122$ form) and r(GC)d(GTATACGC) ($P2_12_12_1$ form), both in the presence of $[Co(NH_3)_6]^{3+}$. It is apparent that A-DNA molecules form crystal lattices by abutting their terminal base pairs onto the shallow and wide minor groove of other A-DNA duplexes. We have first noted this A-DNA binding motif in the crystal structure of the DNA octamer d(GGCCGGCC) (Wang et al., 1982). Subsequent studies confirmed that this type of interaction is indeed ubiquitous among all A-DNA crystal structures.

How do these two different crystal packings influence the local DNA structures? Fig. 4 compares several important helical/local conformational parameters in graph forms. A quick glance of those graphs gives an impression that significant local variations exist. Take the helical twist (Ω) angles as an example. In the $P6_122$ form, the five unique steps have the following Ω values for the d(ACCGGCCGGT) and d(ACCCGCGGGT) decamers, respectively: 33.4°/32.3° (A1pC2/A1pC2), 32.8°/33.9° (C2pC3/C2pC3), 30.9°/28.0° (C3pG4/C3pC4), 36.8°/36.9° (G4pG5/C4pG5), and 32.6°/33.6° (G5pC6/G5pC6). Despite these variations, the averaged Ω values for the d(ACCGGCCGGT) and d(ACCCGCGGGT) decamers are 32.9° and 33.4°, respectively (Table 2), and they are very close to that of the canonical A-DNA (33.3°).

In the $P2_12_12_1$ form, as the two independent DNA strands behave differently, the helix has an asymmetric pattern of the Ω values for the nine unique steps (Fig. 4 *A*). Most of them cluster around 32°, again close to that of the canonical A-DNA. Some steps are rather unusual. In particular the T4pA5 step of r(GC)d(GTATACGC) has a low Ω of 28°, with a compensating larger Ω of 36° for the A5pT6 step.

An interesting question that may be addressed here is whether those local conformational variations are the intrinsic sequence-dependent properties of A-DNA conformation. One way to address this question is to examine a particular sequence in different sequence locations (contexts). A convenient sequence to use for comparison is the CpG steps in different molecules. This step was seen to have an unusually small helical twist angle (Ω) of ~26° in previous studies of octamer A-DNA structures (Wang et al., 1982; Haran et al., 1987). Fig. 5 compares the base-base stacking patterns of six independent CpG steps: C3pG4 in d(ACCGGCCGGT) and C4pG5 in d(ACCCGCGGGT) of the $P6_122$ form plus C3pG4 and C7pG8 in d(ACCGGCCGGT) and rC2pG3 and rC8pG9 in r(GC)d(GTATACGC) of the $P2_12_12_1$ form. It is clear that they have different Ω angles, ranging from 28° to 37° (Fig. 4). In addition, their stacking patterns also vary so that the changing inter-strand G-over-G stackings are apparent. Despite these local variations, their global conformations remain close to canonical A-DNA (Table 2). It appears that the DNA backbone makes appropriate compensations for the variable local conformations to achieve a similar global conformation.

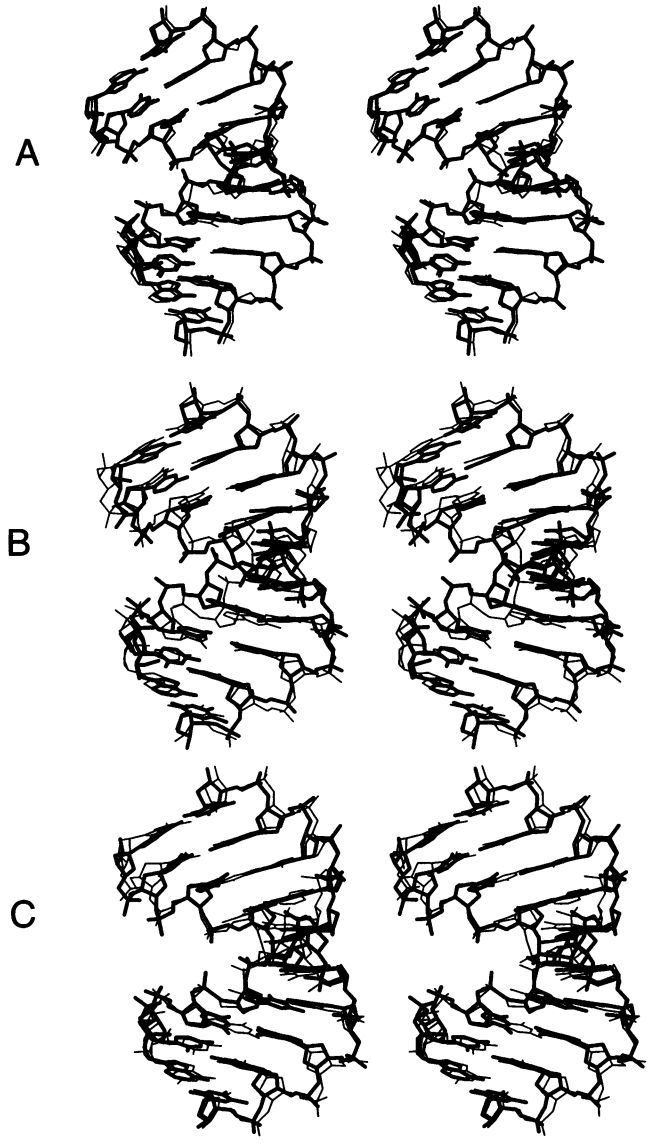

FIGURE 2 Comparisons of the four A-DNA helixes crystallized in two space groups. The rmsd was calculated using all common atoms between two molecules. (*A*) The $P6_122$ form of d(ACCGGCCGGT) versus the $P6_122$ form of d(ACCCGCGGGT) (rmsd = 0.75 Å). (*B*) The $P6_122$ form of d(ACCGGCCGGT) versus the $P2_12_12_1$ form of d(ACCGGCCGGT) (rmsd = 1.61 Å). (*C*) The $P2_12_12_1$ form of d(ACCGGCCGGT) versus the $P2_12_12_1$ form of r(GC)d(GTATACGC) (rmsd = 1.00 Å).

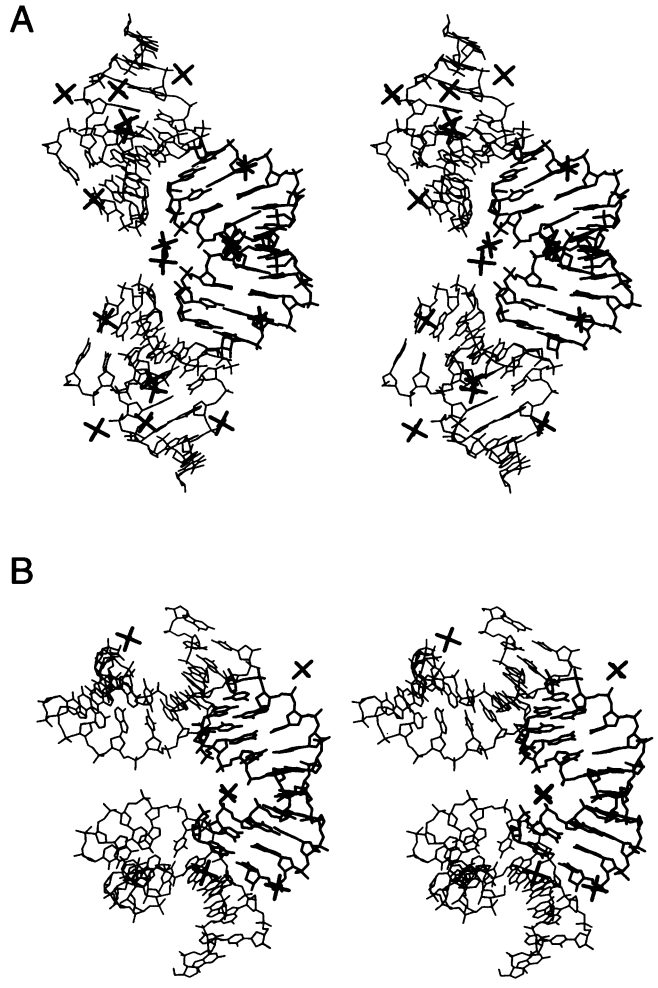

FIGURE 3 Crystal packings of A-DNA duplexes in the presence of $Co(NH_3)_6^{3+}$ ions. (*A*) The $P6_122$ form of d(ACCGGCCGGT). Three symmetry-related duplexes at (x, y, z), $(1 - x, y - x, 2/3 - z)$ and $(-1 + y, x, 1/3 - z)$ are shown. Three independent $Co(NH_3)_6^{3+}$ binding sites are found. (*B*) The $P2_12_12_1$ form of r(GC)d(GTATACGC). Three symmetry-related duplexes at (x, y, z), $(1/2 - x, -y, -1/2 + z)$ and $(-x, 1/2 + y, 1/2 - z)$ are shown. Two independent $Co(NH_3)_6^{3+}$ binding sites are found.

What determines the local conformations? The most obvious factor is a result of the crystal packing interactions. In the $P6_122$ lattice of d(ACCGGCCGGT) and d(ACCCGCGGGT), two terminal A1-T10 base pairs "stack" over the backbone of two symmetry-related duplexes (Fig. 3 *A*). It is interesting that the two molecules use slightly different hydrogen bonding interactions to accomplish the same packing patterns. For d(ACCGGCCGGT), the A1-T10 base pair abuts close to the G4-G5 sequence so that the A1 residue is hydrogen bonded to the N2 positions of G4 and G5 bases from the same strand, whereas for d(ACCCGCGGGT), the A1 residue is hydrogen bonded to the N2 positions of G7 from the opposite strand (Fig. 6, *A* and *B*, and Table 3).

In the $P2_12_12_1$ lattice of d(ACCGGCCGGT), two symmetry-related terminal base pairs, A1-T10 and A11-T20, stack over the backbone near the G14-G15 and G18-G19 sequences, respectively (Fig. 3 *B*). The detailed interactions are shown in Fig. 6, *C* and *D*. Here, four inter-helix hydrogen bonds are found for the A10-T11 base pair, whereas two are found for the A1-T20 base pair (Table 3). Therefore the asymmetric interactions of the decamer duplex with the neighboring duplexes produce a more asymmetric helix in the $P2_12_12_1$ lattice, as evident from the helical parameters shown in Fig. 5. Likewise, in the $P2_12_12_1$ lattice of r(GC)-d(GTATACGC), two symmetry-related terminal base pairs, G1-C10 and G11-C20, pack asymmetrically on neighboring helixes (Fig. 6, *E* and *F*). Table 3 lists the inter-helix hydrogen bonds.

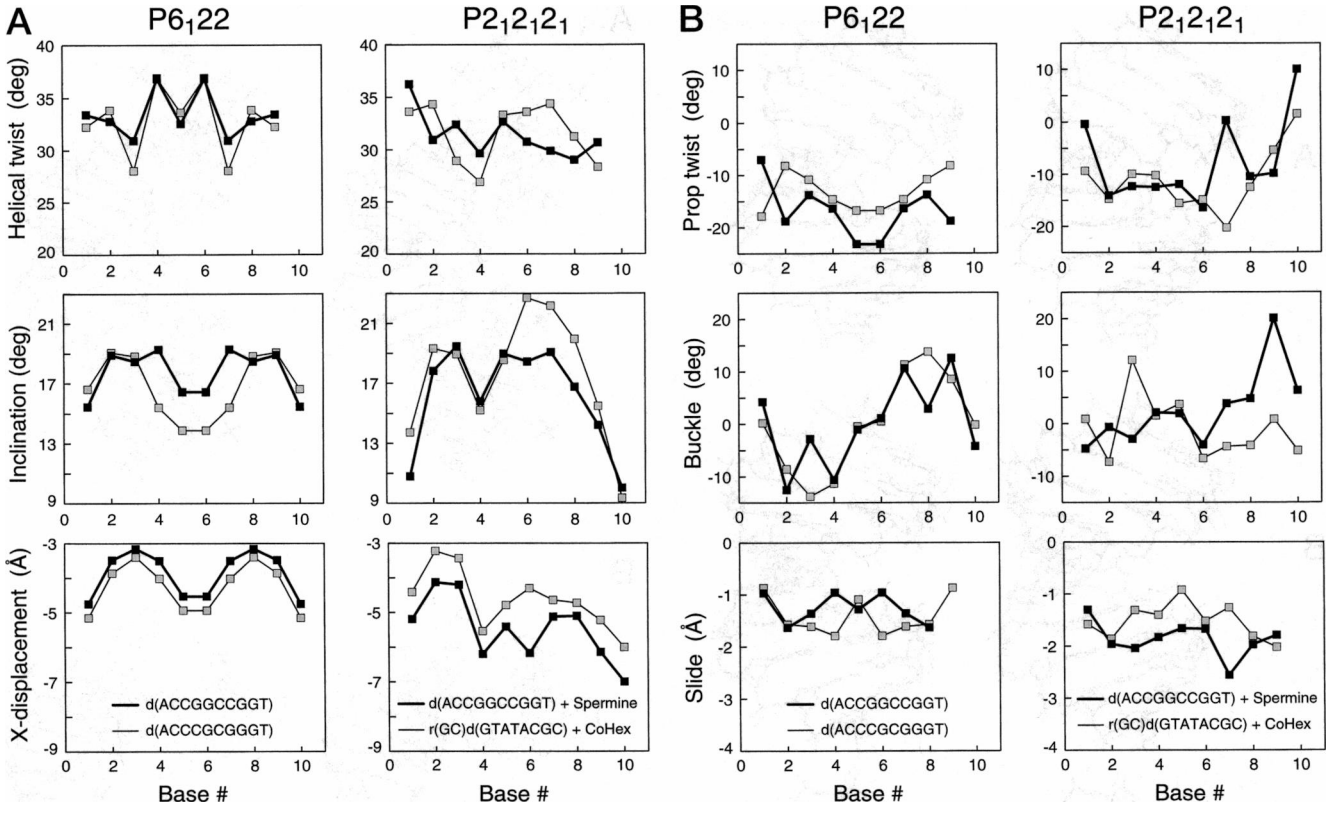

FIGURE 4 Comparisons of the helical parameters of the four independent crystal structures.

Three binding modes of $[Co(NH_3)_6]^{3+}$ to A-DNA

In this work, we show that by changing the choice of metal ions, we were able to induce the same DNA sequence d(ACCGGCCGGT) into two different crystal lattices. Mg^{2+} and $[Co(NH_3)_6]^{3+}$ ions produced the hexagonal form, whereas spermine ion produced the orthorhombic form. In contrast, r(GC)d(GTATACGC) formed only the $P2_12_12_1$ lattice in the presence of a variety of ions, including $[Co(NH_3)_6]^{3+}$ ion. The reason for this is not clear.

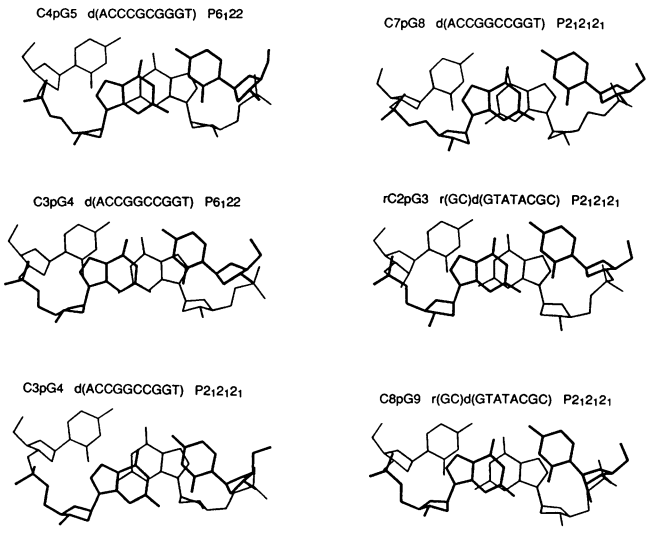

FIGURE 5 Comparisons of the base-base stacking interactions of the six independent CpG steps in four crystal structures.

In the $[Co(NH_3)_6]^{3+}$ forms of both d(ACCGGCCGGT)-$P6_122$ and r(GC)d(GTATACGC)-$P2_12_12_1$ lattices, several bound $[Co(NH_3)_6]^{3+}$ ions were observed in the electron density maps. Fig. 3 shows the locations of them in the lattices. Some of them are found in the interstitial space created by symmetry-related duplexes and they are in contact with the negatively charged phosphate groups. In fact, the two independent $[Co(NH_3)_6]^{3+}$ ions found in the r(GC)-d(GTATACGC)-$P2_12_12_1$ lattice (Fig. 3 *B*) involve only this type of NH_3-phosphate interactions. In the d(ACCGGC-CGGT)-$P6_122$ form, one of the $[Co(NH_3)_6]^{3+}$ ions (denoted Co1) has similar interactions that put the Co1 ion midway across the narrow major groove (Fig. 1 *B*), bridging the phosphates of C3 and C12 residues (Fig. 7 *A*).

A more intriguing type of $[Co(NH_3)_6]^{3+}$-DNA interaction is found in the d(ACCGGCCGGT)-$P6_122$ lattice (Fig. 3 *A*) where three independent $[Co(NH_3)_6]^{3+}$ ions are located (Fig. 1 *B*). The detailed interactions are depicted in Fig. 7. The second $[Co(NH_3)_6]^{3+}$ ion (denoted Co2) is located at the center of the deep major groove near the G4-G5 bases of a duplex (Fig. 1 *B*). However, because of the inherent symmetry of the duplex (coinciding with the crystallographic twofold axis) the same $[Co(NH_3)_6]^{3+}$ ion may bind to the symmetry-related G4*-G5* bases. Yet the two sites

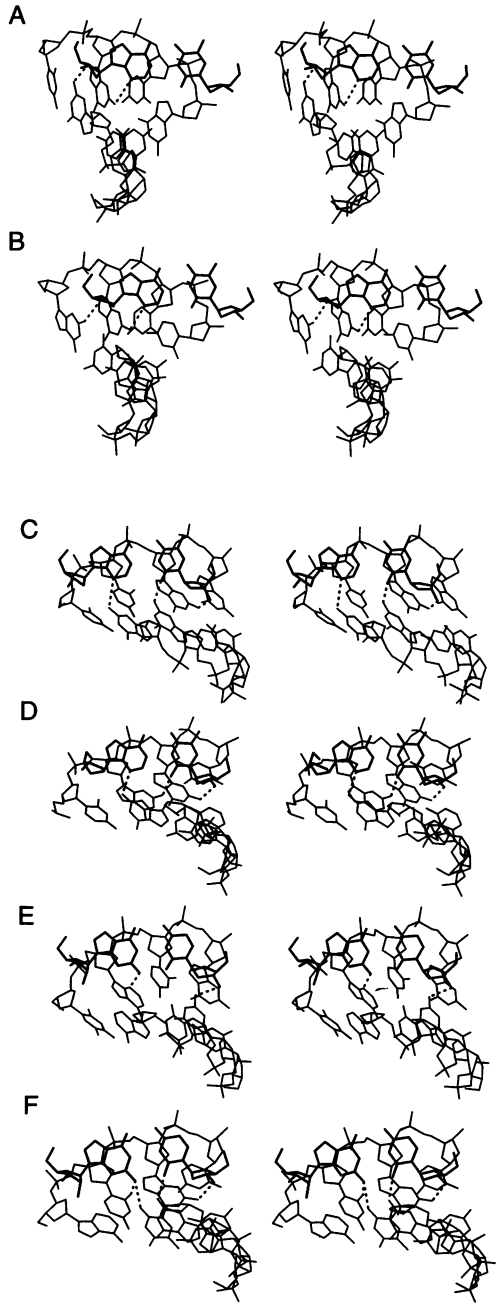

FIGURE 6 Stereoscopic views of the inter-helix hydrogen bonding interactions between the A-DNA duplex and the terminal base pair from the neighboring helix.

TABLE 3 Possible inter-helix hydrogen bonds (distances <3.7 Å) in A-DNA crystals

Atom1----Atom2	Distance (Å)
$P6_122$ form	
d(ACCCGCGGGT)-Ba	
A1O4′----G7N2	3.25
A1N3----G15N2	3.68*
d(ACCGGCCGGT)-CoHex	
A1O4′----G14N2	3.07
A1N3----G15N2	3.29
$P2_12_12_1$ form	
d(ACCGGCCGGT)-Spermine	
A1N3----G15N2	3.25
G4N2----A11N3	2.64
T10O3′----G19N2	2.87
T10O2----G18N2	3.07
G14N2----T20O2	3.00
G18O4′----A11O5′	2.92
T20O3′----G8N2	3.53*
r(GC)d(GTATACGC)-CoHex	
G1N2----A7N3	3.33
G3N2----C10O2	3.23
T4O2----G11N2	2.84
A5O4′----C12O2′	2.67
G11O2′----A17N3	2.85
G11N2----C18O2	3.04

Atom 1 is from the reference helix at (x, y, z) and atom 2 is from the symmetry-related duplexes.
* These distances are too long for good hydrogen bonds.

are too close to each other so that a single $[Co(NH_3)_6]^{3+}$ ion can bind only to a GGCC:CCGG sequence at either of the two sites, but not both at the same time. This creates a disordered binding mode as reflected in the difference Fourier map (Fig. 1 *B*) in which an elongated electron density envelope can be fitted with two closely-spaced $[Co(NH_3)_6]^{3+}$ ions. Another $[Co(NH_3)_6]^{3+}$ ion (denoted Co3) is located near the G8-G9 bases; its detailed interactions are shown in Fig. 7 *C*. In the latter two binding modes, a single $[Co(NH_3)_6]^{3+}$ ion is bound to the edges of two adjacent intra-stranded guanines through hydrogen bonds to the N7 and O6 sites of guanines.

Ba^{2+} bridges two adjacent guanines

In the d(ACCCGCGGGT)-$P6_122$ form, we have located a barium ion (Ba^{2+}) that bridges two adjacent guanines (G7 and G8) by coordination to the N7 and O6 sites of guanines (Fig. 7 *D*). This affirms our earlier observation that the major groove side of the guanine base is the preferred binding site for simple metal ions. The interactions of metal ions Co^{2+}, Cu^{2+}, and Ba^{2+} with DNA in six DNA crystal structures have been studied and they showed that the transition metal ions Co^{2+} and Cu^{2+} coordinate exclusively to the N7 position of guanine bases (Gao et al., 1993). Interestingly, in the Z-DNA crystals, Ba^{2+} ions prefer to coordinate simultaneously with both N7 and O6 positions of guanines from different helixes.

The present mode of Ba^{2+} binding to two intra-stranded guanines is different from that observed in the Z-DNA crystal lattice (Gao et al., 1993) where two guanine bases from neighboring helixes are facing each other so that their N7 and O6 atoms are pointing to the same area, creating a cavity approximately 3 Å in diameter suitable as a Ba^{2+} ion binding site. Therefore, the Ba^{2+} ion has at least two binding modes to DNA, one that binds to two intra-stranded guanines in A-DNA and the other that bridges two Z-DNA helices. Both involve simultaneous coordinations of Ba^{2+} to

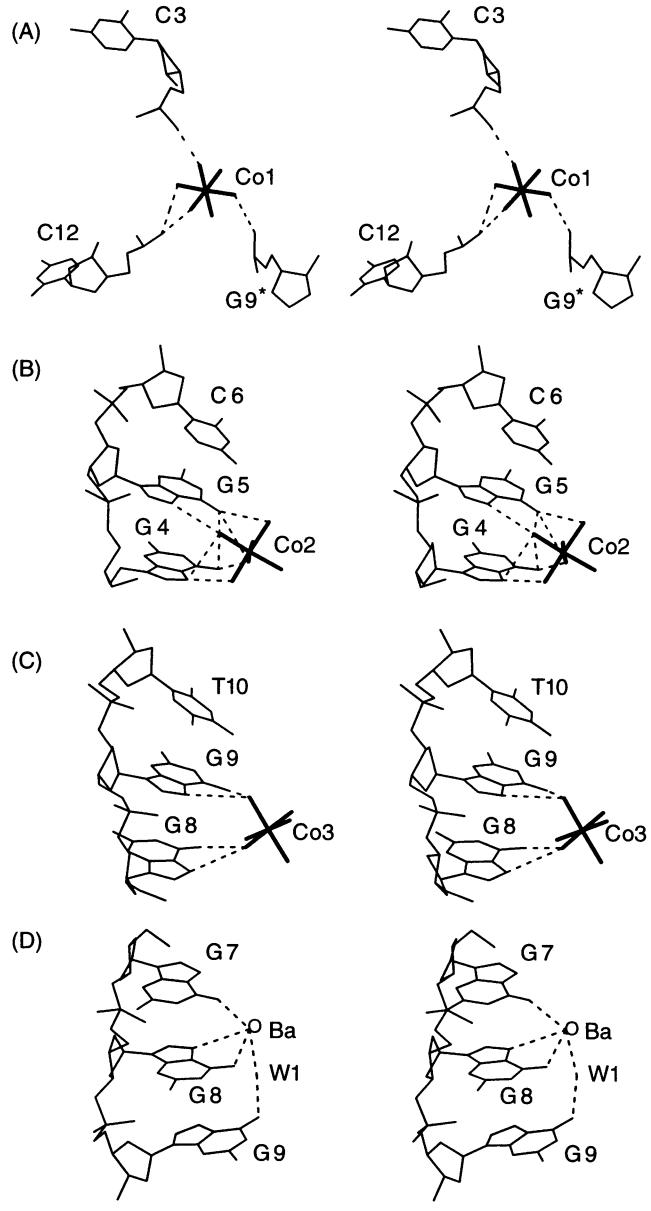

FIGURE 7 Stereoscopic views of the detailed interactions between $[Co(NH_3)_6]^{3+}$ ions and A-DNA in the crystal structure of the $P6_122$ form of d(ACCGGCCGGT). Three different binding modes are found. (*A*) Co1 bridges three phosphate groups. (*B*) Co2 and (*C*) Co3 adhere to the edges of two adjacent guanines. (*D*) Stereoscopic views of the detailed interactions between Ba^{2+} ion and the N7/O6 sites of two adjacent guanines in the crystal structure of the $P6_122$ form of d(ACCCGCGGGT).

the N7 and O6 of guanines. The distances between the Ba^{2+} ion and the N7/O6 atoms vary between 2.82 Å and 3.12 Å.

DISCUSSION

In this paper we have analyzed the A-DNA structures of three different decamer oligonucleotides in two crystal lattices and obtained several interesting conclusions. We showed that, although the overall conformations of all four structures remain very close to canonical A-DNA, the local structure is intimately influenced by the crystal packing environments. For example, the six independent CpG steps in these four structures have different base-base stacking patterns, with their helical twist angles (Ω) ranging from 28° to 37°. These variable local conformations result primarily from the hydrogen bonds between the terminal base pairs of one helix and the base pairs from another helix. (This type of inter-helix base-base interaction, which may be considered as special kinds of base pairs (e.g., base triple), is ubiquitous in A-DNA crystals.) It should be noted that the polymorphic crystal forms of an A-DNA decamer have been compared in the structures of d(GCGGGC-CCGC) and similar conclusions have been drawn (Ramakrishnan and Sundaralingam, 1993a,b).

Such observations of local conformational variability are relevant in understanding the possible function of A-DNA or RNA. A-DNA or RNA are considered to be less flexible than B-DNA. The fact that A-DNA conformation can be modified to some extent by crystal packing interactions suggests that proteins can modulate the conformation of A-DNA/RNA to achieve optimal recognition. This has been elegantly demonstrated in the recent crystal structures of the TBP/TATA-box complex (Kim et al., 1993a,b). Another equally dramatic example of the RNA deformability has been seen in the complex of the MS2 coat protein and the RNA tetra-loop hairpin that is specifically recognized by the coat protein. The stem of the RNA hairpin contains an extra-helical adenine that is stacked within the helix in free RNA but becomes looped out in the protein-RNA complex (Valegard et al., 1994).

The formation of A-DNA is influenced by several factors. It can be induced by low water activity. For example, alcohol facilitates the transition to A-DNA. In the A-DNA decamer crystals, we note that nearly the entire surface of the wide minor groove is occupied by terminal base pairs from other duplexes. Essentially the hydration shell in the A-DNA minor groove is completely displaced by the hydrophobic surface of base pairs. In other words, the A-DNA duplexes in the crystal lattice are embedded in a hydrophobic environment, created by the terminal base pairs from other duplexes. This is consistent with the fact that A-DNA is favored in an environment of low water activity.

Additionally, certain sequences have higher propensity in forming A-DNA. For example, poly(dG)·poly(dC) exists only in the A conformation (Benevides et al., 1986). Inspection of Table 2 indicates that A-DNA structures are favored by DNA with GpG sequences or by the incorporation of the RNA backbone (i.e., an RNA·DNA chimera). It has been suggested that the stacking interactions of the GpG step is conducive for A-DNA (Wang et al., 1982; McCall et al., 1986), although the theoretical basis for this remains to be worked out.

Despite the frequent observations of A-DNA in oligonucleotide crystals, determination of A-DNA structure in solution (e.g., by NMR) has proven to be elusive. Some of the DNA oligomers that have been crytallized in the A form, when studied by NMR, showed that they are predominantly

in the B-DNA conformation (e.g., C2′-endo sugar pucker) in solution (Clark et al., 1990). Recently it has been shown that $[Co(NH_3)_6]^{3+}$ induces the A-DNA structure for DNA with stretches of GpG sequences as is evident, among other data, by the characteristic changes in their circular dichroism spectra (Braunlin and Xu, 1992; Xu et al., 1993). More recently we have demonstrated that $[Co(NH_3)_6]^{3+}$ induces a 34-mer DNA duplex $[d(A_2G_{15}C_{15}T_2)]_2$, which is more than three full turns of double helix, from B-DNA to A-DNA by NMR (Robinson et al., unpublished data). The binding sites on DNA for $[Co(NH_3)_6]^{3+}$ have also been identified. Our NMR data revealed direct NOE cross-peaks between the NH_3 protons of $[Co(NH_3)_6]^{3+}$ and the DNA protons, including GH8, GH1 (imino), and CH4 (amino) protons. This clearly suggests that $[Co(NH_3)_6]^{3+}$ adheres to guanine bases in the deep major groove of the double helix. This is completely consistent with the crystal structure of d(ACCGGCCGGT) in complex with $[Co(NH_3)_6]^{3+}$ ions shown in Fig. 1 *B*. A major binding mode (Fig. 2) is with $[Co(NH_3)_6]^{3+}$ ions located in the major groove of the decamer A-DNA duplex at the G4pG5 and the G8pG9 steps. Such a binding mode (i.e., $[Co(NH_3)_6]^{3+}$ ions binding at the GpG sites) has been observed in the 3-Å resolution structure of yeast phenylalanine tRNA crystals (Hingerty et al., 1982).

It is interesting to mention that $[Co(NH_3)_6]^{3+}$ is extremely potent in promoting, at submicromolar concentration, the B- to Z-DNA transition for poly-d(m^5C-G) (Behe and Felsenfeld, 1981; Peck et al., 1982). It is equally effective in promoting the formation of the DNA four-way junction (Holliday junction) (Duckett et al., 1990). More recently, it has been shown that the activity of a hammerhead ribozyme (whose crystal structure has been determined recently (Pley et al., 1994)) is strongly dependent on the Mg^{2+} concentration and $[Co(NH_3)_6]^{3+}$ can substitute for Mg^{2+} effectively (Bassi et al., 1995). Therefore, $[Co(NH_3)_6]^{3+}$ is a novel ion that is useful in the study of the function of nucleic acids.

The interactions of $[Co(NH_3)_6]^{3+}$ with Z-DNA have been studied by x-ray diffraction, which showed that $[Co(NH_3)_6]^{3+}$ bridges a guanine base (at N7/O6 sites) and the 3′-phosphate group by hydrogen bonds (Gessner et al., 1985). The binding of other analogous metal ion-amine complexes to nucleic acids have also been characterized. The binding modes of $[Ru(NH_3)_6]^{3+}$ to Z-DNA (Ho et al., 1987) and $[Rh(NH_3)_6]^{3+}$ to RNA (Cruse et al., 1995) have been studied by x-ray crystallography. Therefore, $[Co(NH_3)_6]^{3+}$ and related ions are able to stabilize alternative DNA conformations by providing a very effective hydrogen bonding network and a high positive charge density (+3) for the neutralization of negatively charged phosphates in DNA/RNA. In this respect, $[Co(NH_3)_6]^{3+}$ is similar to the biologically relevant polyamines such as spermine and spermidine. The latter molecules are also capable of promoting the B- to Z-DNA transition effectively (Behe and Felsenfeld, 1981; Peck et al., 1982). In the crystal structure of the $P2_12_12_1$ form of d(ACCGGCCGGT) A-DNA crystals, only spermine was used as the major counter ion (except the sodium cacodylate buffer). However, no spermine molecule could be located unambiguously. This is in contrast to the analysis of the crystal strcuture of the RNA·DNA chimera r(C)d(CGGCGCCG)r(G) (Ban et al., 1994b) in which a spermine molecule in an extended conformation was found to bind only to phosphate groups.

From Fig. 1 *B* it is clear that, even though the size of the $[Co(NH_3)_6]^{3+}$ ion is ~8 Å in diameter, comparable with the width of the narrow major groove opening of A-DNA, the edges of the base pairs are still accessible to a bulky ligand like $[Co(NH_3)_6]^{3+}$. Our results from the NMR studies of several DNA oligonucleotides, including the 34-mer duplex, indicate that $[Co(NH_3)_6]^{3+}$ can enter the deep groove of the A-DNA duplex (Robinson et al., unpublished data). Paradoxically, other recent data suggested that the accessibility of the major groove in RNA (therefore A-DNA) is limited (Weeks and Crothers, 1993).

The binding mode of the Ba^{2+} ion to guanine bases is interesting. We have shown previously that GN7 is the preferred binding site for many transition metal ions such as Co^{2+}. We believe that in A-DNA, or RNA, the binding of the small metal ions (e.g., Co^{2+} and Ni^{2+}), along with their hydration shell, at the GN7 sites, (which are buried in the very deep and narrow major groove) would generate unfavorable contacts and destabilize the DNA helix, as shown before (Jia and Marzilli, 1991). However, a larger metal ion such as Ba^{2+} or Pb^{2+} may bind to the guanine N7/O6 sites without significantly affecting the DNA/RNA structure. Note that Pb^{2+} ion is unusual in that it is capable of catalyzing the breakage of the RNA backbone (Behlen et al., 1990). The binding mode of the Ba^{2+} ion to guanine bases may be useful in understanding the interactions of other DNA structures, e.g., G-quartet, stabilized by Ba^{2+} (Laughlan et al., 1994).

This work was supported by National Institutes of Health grants GM-41612 and CA-52506 (A. H.-J. W).

REFERENCES

Baeyens, K. J., H. De Bondt, and S. R. Holbrook. 1995. Structure of an RNA double helix including uracil-uracil base pairs in an internal loop. *Nature Struct. Biol.* 2:56–62.

Ban, C., B. Ramakrishnan, and M. Sundaralingam. 1994a. A single 2′-hydroxyl group converts B-DNA to A-DNA: crystal structure of the DNA-RNA chimeric decamer duplex d(CCGGC)r(G)d(CCGG) with a novel intermolecular G·C base-paired quadruplet. *J. Mol. Biol.* 236: 275–285.

Ban, C., B. Ramakrishnan, and M. Sundaralingam. 1994b. Crystal structure of the highly distorted chimeric decamer r(C)d(CGGCGCCG)r(G)· spermine binding to phosphate only and minor groove tertiary base-pairing. *Nucleic Acids Res.* 22:5466–5476.

Bassi, G. S., N.-E. Mollegaard, A. I. H. Murchie, E. von Kitzing, and D. M. J. Lilley. 1995. Ionic interactions and the global conformations of the hammerhead ribozyme. *Nature Struct. Biol.* 2:45–55.

Behe, M., and G. Felsenfeld. 1981. Effects of methylation on a synthetic polynucleotide: the B-Z transition in poly(dG-m^5dC)·poly(dG-m^5dC). *Proc. Natl. Acad. Sci. USA.* 78:1619–1623.

Behlen, L. S., J. R. Sampson, A. B. DiRenzo, and O. C. Uhlenbeck. 1990. Lead-catalyzed cleavage of yeast $tRNA^{Phe}$ mutants. *Biochemistry*. 29: 2515–2523.

Benevides, J. M., A. H.-J. Wang, A. Rich, Y. Kyogoku, G. A. van der Marel, J. H. van Boom, and G. J. Thomas, Jr. 1986. Raman spectra of single crystals of r(GCG)d(CGC) and d(CCCCGGGG) and models for A DNA, their structure transitions in aqueous solution, and comparison with double-helical poly(dG)·poly(dC). *Biochemistry*. 25:41–50.

Bingman, C. A., G. Zon, and M. Sundaralingam. 1992. Crystal and molecular structure of the A-DNA dodecamer d(CCGTACGTACGG): choice of fragment helical axis. *J. Mol. Biol.* 227:738–756.

Braunlin, W. H., and Q. Xu. 1992. Hexaamminecobalt(III) binding environments on double-helical DNA. *Biopolymers*. 32:1703–1711.

Clark, G. R., D. G. Brown, M. Sanderson, T. Chwalinsky, S. Neidle, J. M. Veal, R. L. Jones, W. D. Wilson, G. Zon, E. Garman, and D. I. Stuart. 1990. Crystal and solution structure of the oligonucleotide $d(ATGCGCAT)_2$: a combined x-ray and NMR study. *Nucleic Acids Res.* 18:5521–5528.

Cruse, W. B. T., P. Saludjian, E. Biala, P. Strazewski, T. Frange, and O. Kennard. 1995. Structure of the mispaired RNA double helix at 1.6 Å resolution and implications for the prediction of RNA secondary structure. *Proc. Natl. Acad. Sci. USA*. 91:4160–4164.

Dock-Bergeon, A. C., B. Chevrier, A. Podiarny, J. Johnson, J. S. de Bear, G. R. Grough, P. T. Gilham, and D. Moras. 1989. Crystallographic structure of an RNA helix: $[U(UA)_6A]_2$. *J. Mol. Biol.* 209:459–474.

Duckett, D. R., A. I. H. Murchie, and D. M. J. Lilley. 1990. The role of metal ions in the conformation of the four-way DNA junctions. *EMBO J.* 9:583–590.

Egli, M., N. Usman, and A. Rich. 1993. Conformational influence of the ribose 2′-hydroxyl group: crystal structures of DNA-RNA chimeric duplexes. *Biochemistry*. 32:3221–3237.

EMBO Workshop. 1989. Definitions and nomenclature of nucleic acid structure parameters. *EMBO J.* 8:1–4.

Frederick, C. A., G. J. Quigley, M.-K. Teng, M. Coll, G. A. van der Marel, J. H. van Boom, A. Rich, and A. H.-J. Wang. 1989. Molecular structure of an A-DNA decamer d(ACCGGCCGGT). *Eur. J. Biochem.* 181: 295–307.

Gao, Y.-G., M. Sriram, and A. H.-J. Wang. 1993. Crystallographic studies of metal ion DNA interactions: different binding modes of cobalt(II) and barium(II) to N-7 of guanines in Z-DNA and a drug DNA complex. *Nucleic Acids Res.* 21:4093–4101

Gessner, R. G., G. J. Quigley, A. H.-J. Wang, G. A. van der Marel, J. H. van Boom, and A. Rich. 1985. Structural basis for stabilization of Z-DNA by cobalt hexaammine and magnesium cations. *Biochemistry*. 24:237–250.

Haran, T. E., Z. Shakked, A. H.-J. Wang, and A. Rich. 1987. The crystal structure of d(CCCCGGGG): a new A-form variant with an extended backbone conformation. *J. Biomol. Struct. Dyn.* 5:199–217.

Heineman, U., C. Alings, and M. Bansal. 1992. Ligand binding potential of a G/C stretch in B-DNA. *EMBO J.* 11:1931–1939.

Hendrickson, W. A., and J. Konnert. 1979. Biomolecular Structure, Conformation, Function and Evolution. R. Srinvasan, editor. Pergamon, Oxford. 43–57.

Hingerty, B. E., R. S. Brown, and A. Klug. 1982. Stabilization of the tertiary structure of yeast phenylalanine tRNA by $[Co(NH_3)_6]^{3+}$. *Biochim. Biophys. Acta*. 697:78–83.

Ho, P. S., C. A. Frederick, D. Saal, A. H.-J. Wang, and A. Rich. 1987. The interactions of ruthenium hexaammine with Z-DNA: crystal structure of a $Ru(NH_3)_6$3+ salt of d(CGCGCG) at 1.2 Å resolution. *J. Biomol. Struct. Dyn.* 4:521–534.

Jia, X., and L. G. Marzilli. 1991. Zinc ion-DNA polymer interactions. *Biopolymers*. 31:23–44.

Kim, Y. C., J. H. Geiger, S. Hahn, and P. B. Sigler. 1993a. Crystal structure of a yeast TBP TATA-box complex. *Nature*. 365:512–520.

Kim, J. L., D. B. Nikolov, and S. K. Burley. 1993b. Co-crystal of TBP recognizing the minor groove of a TATA element. *Nature*. 365: 520–527.

Laughlan, G., A. I. H. Murchie, D. G. Norman, M. H. Moore, P. C. E. Moody, D. M. J. Lilley, and B. Luisi. 1994. The high-resolution crystal structure of a parallel-stranded guanine tetraplex. *Science*. 265:520–524.

McCall, M., T. Brown, W. N. Hunter, and O. Kennard. 1986. The crystal structure of d(GGATGGGAG) forms an essential part of the binding site for transcription factor IIIA. *Nature*. 322:661–664.

Peck, L. J., A. Nordheim, A. Rich, and J. C. Wang. 1982. Flipping of cloned d(pCpG)n·d(pCpG)n DNA sequences from right- to left-handed helical structure by salt, Co(III), or negative supercoiling. *Proc. Natl. Acad. Sci. USA*. 79:4560–4564.

Pley, H. W., K. M. Flaherty, and D. B. McKay. 1994. Three-dimensional structure of a hammerhead ribozyme. *Nature*. 372:68–74.

Ramakrishnan B., and M. Sundaralingam. 1993a. Evidence for crystal environment dominating base sequence effects on DNA conformation: crystal structures of the orthorhombic and hexagonal polymorphs of the A-DNA decamer d(GCGGGCCCGC) and comparison with their isomorphous crystal structures. *Biochemistry*. 32:11458–11468.

Ramakrishnan B., and M. Sundaralingam. 1993b. High resolution crystal structure of the A-DNA decamer d(CCCGGCCGGG): novel intermolecular base paired G*(G·C) triplets. *J. Mol. Biol.* 231:431–444.

Sauer, R. 1995. Minor groove DNA recognition by α-helices. *Nature Struct. Biol.* 2:7–9.

Shakked, Z., D. Rabinovich, O. Kennard, W. B. T. Cruse, S. A. Salibury, and M. A. Viswamitra. 1983. Sequence-dependent conformation of an A-DNA double helix: the crystal structure of the octamer d(G-G-T-A-T-A-C-C). *J. Mol. Biol.* 166:183–201.

Sinden, R. R. 1994. DNA Structure and Function. Academic Press, San Diego.

Steitz, T. A. 1990. Structural studies of protein-nucleic acid interaction: the sources of sequence-specific binding. *Q. Rev. Biophys.* 23:205–280.

Valegard, K., J. B. Murphy, P. G. Stockley, N. J. Stonehouse, and L. Liljas. 1994. Crystal structure of an RNA bacteriophage coat protein-operator complex. *Nature*. 371:623–626.

Verdaguer, N., J. Aymami, D. Fernandez-Forner, I. Fita, M. Coll, T. Huynh-Dihn, J. Iglon, and J. A. Subirana. 1991. Molecular structure of a complete turn of A-DNA. *J. Mol. Biol.* 221:623–635.

Wang, A. H.-J., S. Fujii, J. H. van Boom, and A. Rich. 1982. Molecular structure of the octamer d(G-G-C-C-G-G-C-C): modified A-DNA. *Proc. Natl. Acad. Sci. USA*. 79:3968–3972.

Wang, A. H.-J., and Y.-G. Gao. 1990. Crystallization of oligonucleotides and their complexes with antitumor drugs. *Methods*. 1:91–99.

Weeks, K. M., and D. M. Crothers. 1993. Major groove accessibility of RNA. *Science*. 261:1574–1577.

Westhof, E., P. Dumas, and D. Moras. 1985. Crystallographic refinement of yeast aspartic acid transfer RNA. *J. Mol. Biol.* 184:119–145.

Xu, Q., R. K. Schoemaker, and W. H. Braunlin. 1993. Induction of B-A transitions of deoxyoligonucleotides by multivalent cations in dilute aqueous solution. *Biophys. J.* 65:1039–1049.